

# Experimental study of the wave generation around a ship bow wave at different scales

*Fabrizio Pistani*<sup>1,2</sup>, *A. Olivieri*<sup>1</sup>, *E.F. Campana*<sup>1</sup>

1. INSEAN, *Italian Ship Model Basin - Resistance & Optimization Dept.*

2. UWA, *University of Western Australia - School of Oil and Gas Engineering.*

fpistani@oil-gas.uwa.edu.au

## Introduction

In the prediction of the performances of a ship, full scale resistance is obtained from model basin tests through the use of corrective coefficients, because not all the physical phenomena can be scaled in the same way. The standard choice is to perform model tests at the same Froude number as the real scale:  $Fr = v^2/\sqrt{g \cdot L}$ . In this way it is ensured that all gravitational related phenomena are correctly scaled and the real and scaled far field wave pattern are in geometrical similarity with the same ratio as the scale coefficient  $\lambda$ . In this approach besides the viscous forces, all the wave breaking related phenomena are not scaled. The limitations in dimensions of the basins for model test do not allow usually to test models whose wave pattern contains breaking waves. The scaling of the wave related phenomena has always been an issue in hydrodynamics and naval research. In the review of Brocchini & Peregrine [1] the lack of detailed experimental results is made clear. Data taken in the real case and model techniques, both numerical and experimental, could be integrated with measurements obtained in intermediate cases. The work here presented aimed to built an experiment closer to reality in its physics but still performed in a controlled environment such as a laboratory. A comparative study at three different scales

of the same model is presented focusing in particular on the bow wave breaking modalities. Measurements of the resistance drag force are also presented.

## Set up

The experiments have been conducted in the INSEAN basin number 1 ( $470 \times 13.5 \times 6.5m$ ). The towing carriage is capable of speeds up to  $14 m/s$  with resolution of  $10^{-3} m/s$ . The geometry chosen for the experiments is the DDG51 hull, representative of a class of slender hull frigates with transom stern, a bulb of modern conception and capable of relatively high speeds. Furthermore the same geometry has been widely investigated around the world and an extensive database is available for scientific purposes [2]. Three geosym models of this hull with scale ratios of  $\lambda = 46.59$  (C2385),  $\lambda = 24.82$  (C2340),  $\lambda = 14.32$  (C2469), have been used in our experiment and tested in a full range of Froude numbers. Their scales chosen in order to have a complete range of generated wavelengths and to obtain the different breaking scenarios. The largest one conceived as the largest possible model in order to avoid significant blockage effects in the basin. Preliminary calculations on the expected wavelength, based on previous experiments [3], had ensured that the generated bow wave was going to be in the range of gravitational waves [4]. The tests have been run in calm

water conditions as specified by the ITTC procedures [5].

### Qualitative observations

A full set of pictures of the breaking bow wave have been taken during the towing of the models, shown in figure 1 are the bow pictures relative to the velocity correspondent to  $Fr = 0.35$ , chosen for comparing the results.

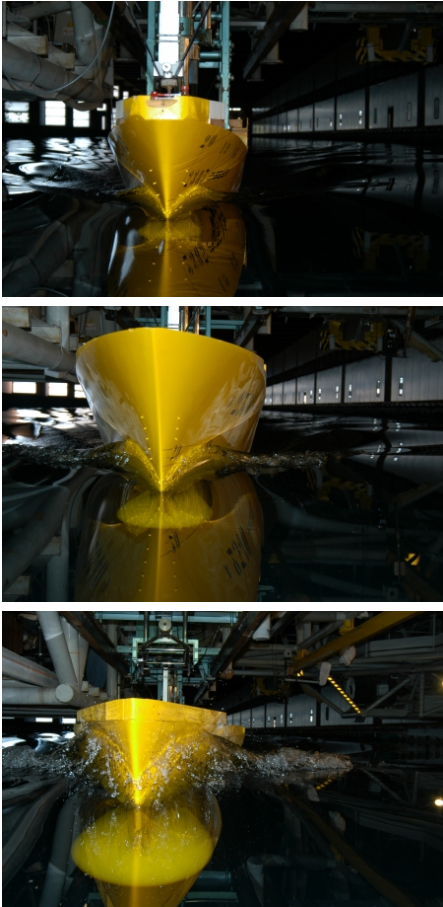


Figure 1: Froude 0.35. From top to bottom: models C.2385, C.2340B, C.2469.

For small scales the influence of the surface tension smooths the water surface, the waves have rounded crests, no air entrainment is present and no air bubbles are seen emerging downstream in the wake. Thus the bow wave of the smallest model (top)

is deeply influenced by surface tension, the bulge of the wave has a smooth appearance and a train of a capillary waves (visible when zooming the picture), is riding in front of the wave crest further away from the hull's side. At increased model length (middle) the bow wave shows a breaking with a crest that goes through an overturning motion close to the inclined surfaces of the bow. The regular capillary wave train seems to be cancelled by the increased turbulent activity at the main crest but a full cavity has not yet formed under the wave crest. Bubbles are seen in the wake of the crest because of the air entrapped, but still no significant water drops are projected forward.

The scenario is quite different for the largest model ( $L_{PP} = 9916 \text{ mm}$ ). As the wave length increases surface tension effects are relatively decreased and the main and only restoring force becomes the gravity. When the wave length is one meter or more we can consider the waves as pure gravity waves. The bow wave in this case is in the range of pure gravity waves and influence of surface tension is limited to those regions with large curvature. The crest of the wave assumes the typical turbulent aspect seen in full scale: furthermore, a considerable amount of air is entrained under the crest and then entrapped into the water, conferring to the breaking wave its characteristic white aspect. The crest overturns and produces secondary ejections when impacts the water surface ahead. All along the crest length there are numerous ejections of drops and jets.

### Resistance results

The resistance force has been measured from  $Fr = 0.05$  to  $Fr = 0.45$ . Repeated runs

have been performed for  $Fr = 0.28$ , i.e. the design speed of the ship;  $Fr = 0.35$ , the condition chosen for the bow wave comparison between the different scales; and  $Fr = 0.41$ , the “flank” speed. The data have been used for uncertainty assessment.

In figure 2 the plots of the total resistance coefficient are shown.  $C_T$  is calculated as usual from the measured total resistance force  $R_T$ :

$$C_T = \frac{R_T}{\frac{1}{2}\rho v^2 S}, \quad (1)$$

where  $S$  is the wetted surface,  $v$  is the velocity of the model,  $\rho$  the density of the water, whereas, following the recommended procedures (ITTC 1978 and 1957), the frictional resistance coefficient  $C_F$  and the residual resistance coefficient  $C_R$  can be calculated as follows:

$$C_F = \frac{0.075}{(\log Re - 2)^2}, \quad (2)$$

$$C_R = C_T - C_F(1 + k). \quad (3)$$

At the low velocities most of the resis-

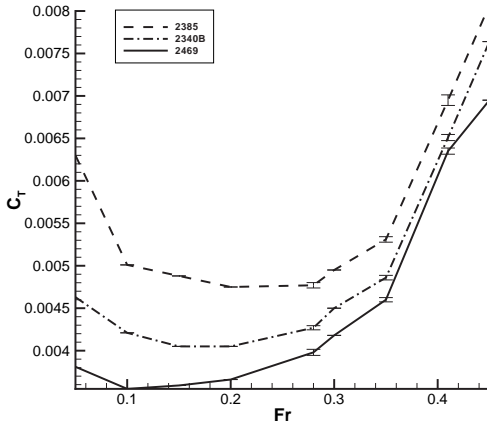


Figure 2:  $C_T$  for the three model scales  $C_{2385}$  ( $\lambda = 46.59$ ),  $C_{2340}$  ( $\lambda = 24.82$ ),  $C_{2469}$  ( $\lambda = 14.32$ ). Error bars correspond to uncertainty in the data at  $Fr=0.28, 0.35, 0.41$ .

tance is due to viscous effects and the large model is the only one that is going to have a fully developed turbulent boundary layer as its Reynolds number already overcomes the critical value. The small model, even if equipped with turbulence stimulators, does not have enough velocity neither is long enough to reach a high enough Reynolds number along its hull surface at low  $Fr$ .

When increasing the Froude numbers the plots of  $C_R$  (fig. 3) relative to the two larger models will take larger values in correspondence to the inception of a stable breaking in the near field waves.

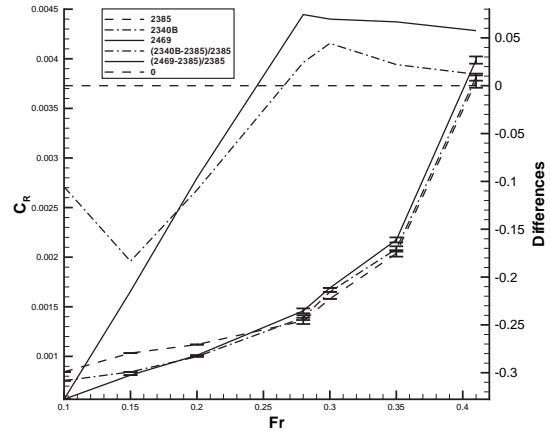


Figure 3:  $C_R$  (left axis) with error bars at  $Fr=0.28, 0.35, 0.41$ . Offset relative to the values of  $C_{2385}$  (right axis) calculated as  $\frac{C_{R(C.2340)} - C_{R(C.2385)}}{C_{R(C.2385)}}$  and  $\frac{C_{R(C.2469)} - C_{R(C.2385)}}{C_{R(C.2385)}}$ .

In the lower range of Froude numbers the slope of the resistance plot relative to the small model is the lowest. Also the slope of the plot relative the middle model is smaller in comparison with the large one.

The plot relative to the small model increases its slope after Froude 0.28 and becomes parallel with the other two plots. Its value is then lower than the resistance of the other two models. The slope of the

middle model behaves the same but earlier, about the value of  $Fr = 0.2$ . It is in this Froude range that the bow wave relative to the two smaller models becomes a fully breaking wave. In the case of the large model, the breaking of the bow wave is relevant since the lowest values of  $Fr$ , thus the slope of its  $C_R$  is the largest of the three from the beginning.

It is the inception of the breaking that influences the change in slope of the  $C_R$  plots. And it happens before on the larger and then on the smaller models because of the different wavelength and absolute values of the velocity. Additional measurements with increased resolution in this range of Froude could detail more quantitatively this change in behavior of the  $C_R$  plot and relate it precisely to the inception of breaking.

### Conclusions

The difference in the resistance coefficients between geosym models is not predicted by current ITTC practice and it can presumably be ascribable to the difference in the wave breaking modalities at the different scales. In the case of a ship advancing in calm water, part of the energy spent is transferred to the body of water in form of wave generation and dissipated in the near field through the wave breaking. Far field wave pattern is not in breaking conditions and in regime of Froude's similarity is geometrically similar from one scale to the other. The contribution to the wave resistance due to the breaking has been estimated in a 15% of the total wave resistance [6]. This affects the scaling up or model to ship resistance measurements. A paper in preparation will integrate the resistance results with measurements of the wave elevation pattern and

of the flow velocity under the breaking wave in an attempt to characterize quantitatively the main differences due to the dimension of the waves.

The authors wish to thank Fred Stern (U. Iowa) for his continuous help. His advice and discussion helped us substantially.

### References

- [1] Brocchini M., Peregrine D.H. (2001) "*The dynamics of strong turbulence at free surfaces. Part 2. The boundary conditions*". J.Fluid Mech. 449, 255-290.
- [2] Stern F., Longo J., Penna R., Olivieri A., Ratcliffe T., Coleman H., (2000). "*International Collaboration On Benchmark Cfd Validation Data For Surface Combatant Dtm Model 5415*". Proc. of the 23rd symposium on naval hydrodynamics, Val de Reuil, France.
- [3] Olivieri A., Pistani F., Avanzini A., Stern F., Penna R. (2001). "*Towing tank experiments of resistance, sinkage and trim, boundary layer, wake, and free surface flow around a naval combattant INSEAN 2340 model*". IIHR Tech. rep. n 421 - Sep 2001. The University of Iowa, Iowa City, USA.
- [4] Duncan J.H. (2001). "*Spilling breakers*". Annual review of fluid mechanics, vol.33 pp.519-547, Annual Reviews inc.
- [5] ITTC Recommended Procedures. (1999) "*Testing and Extrapolation Methods Resistance Resistance Test*". International Towing Tank Conference.
- [6] Larsson L., Baba E. (1996). "*Ship resistance and flow computations*". Advances in marine hydrodynamics, vol.5 pp.1-75, Computational Mechanics Publications, Southampton.

**Pistani, F., Olivieri, A., Campana, E.F.**

**'Experimental study of the wave generation around a ship now wave at different scales'**

**Discusser - J.N. Newman**

Do you have an opinion, regarding the dramatic difference in bow waves of the different models, if this is primarily due to the difference in the Reynolds number or the Weber number?

**Reply:**

It is the  $\lambda$  of the generated wave that changes the overall behaviour of the breaking crest. It has been shown also by 2D numerical simulations that waves with sufficient  $\lambda$  display an overturning crest that at smaller  $\lambda$  is inhibited by surface tension and the crest breaks without overturn. (Iafrafi might have comments on this since he did these computations.) In our experiments the  $Re$  of the three models is above the critical values for the chosen comparison velocity ( $Fr = 0.35$ ).